Bulgarian Chemical Communications, Volume 47, Number 2 (pp. 714 – 719) 2015

Room temperature decomposition of hydrazine catalyzed by nickel oxide nanoparticles

F. Chekin*, S. Sadeghi

Department of Chemistry, Ayatollah Amoli Branch, Islamic Azad University, Amol, Iran

Received April 27, 2014, Revised September 1, 2014

In this work, we report a simple low-cost procedure to synthesize nickel oxide nanoparticles (NiO-NPs) by using sodium dodecyl sulphate (SDS) and gelatin as stabilizer. The synthesized NiO-NPs were characterized by transmission electron microscopy (TEM), powder X-ray diffraction (XRD), scanning electron microscopy (SEM) and UV-vis spectroscopy. The results showed that NiO nanoparticles with high crystallinity can be obtained using this simple method. The grain size measured by TEM was 16 nm in the presence of SDS, which agrees well with the XRD data. SDS plays an important role in the formation of the NiO nanoparticles. Further, the NiO nanoparticles were used as a solid-phase catalyst for the decomposition of hydrazine hydrate at room temperature. The decomposition process was monitored by UV–vis analysis. The present study showed that the nanoparticles were not poisoned after their repeated use in decomposition of hydrazine. It was found that hydrazine was catalytically decomposed to hydrogen and nitrogen gases by the resultant nickel oxide nanoparticles. The decomposition rate at 25 °C was 9.1 nmol/(min mg of NiO-NPs).

Keywords: nickel oxide nanoparticles, sodium dodecyl sulphate, hydrazine, gelatin, catalyst.

INTRODUCTION

Nowadays, synthesis and study of materials consisting of nanometer-sized particles are the subjects of intense research. Reduction of the particle size to the nanometer scale leads to a quantitative change in physical and chemical properties [1-3]. Nanoparticles in crystalline as well as in amorphous phase have important applications in magnetic recording, solar energy transformation, magnetic fluids, electronics, and chemical catalysis [4-12].

Nickel nanoparticles have attracted much attention because of their use in catalysis, medical diagnostics and magnetic applications. A number of techniques have been used for the preparation of nickel nanomaterials, such as chemical vapor deposition (CVD) [13], wet chemical method [14], laser-driven aerosol [15], hydrothermal method [16], and microemulsion [17].

ver the years, attempts have been made to prepare, stabilize and isolate homogeneously dispersed nanoparticles with and without capping agents [18,19]. Upon agglomeration, these particles lose their nanosizes and corresponding properties. In the last few years, extensive structural, kinetic and thermodynamic studies have been performed to explore the fundamental understanding of surfactant–water systems including the effect of additives on micellization [20, 21]. However, there are still conflicting opinions on some aspects, particularly regarding factors controlling the synthesis and stabilization of nanoparticles in aqueous surfactant solutions. Therefore, it is quite difficult to scale up a general method for nanoparticles synthesis using surfactants, because numerous parameters with different influences enter into consideration, while studying a particular system.

Surfactants are amphiphilic in nature. They have two ends with different polarities, and form aggregates, such as micelles, where the hydrophobic tails form the core of the aggregate and the hydrophilic heads are in contact with the surrounding liquid. Surfactants can serve as a capping or protecting agent for nanoparticles against external forces [22,23]. The kinetics and morphology of nanomaterials can be either accelerated or changed, depending on the nature of the reducing agents and the surfactant. The surfactants not only provide favorable sites for the growth of the particle assemblies but also influence the formation process, as well as the chemical properties of the particulate guests, thus unfolding novel chemistries [24].

Hydrazine (N_2H_4) is widely used as (i) a high–energy propellant in rockets and spacecrafts by the military and aerospace industries; (ii) a powerful reducing agent for zero–emission fuel cells [25,26].

---

* To whom all correspondence should be sent:
E-mail: fchekin@yahoo.com
Tel.: +98 121 2517000; Fax: +98 121 2517043

Electro–oxidation of N_2H_4 is the basis of an established fuel cell, due to its high capacity and lack of contamination. However, N_2H_4 is toxic and can be readily absorbed by oral, dermal or inhalation routes of exposure [27]. It is therefore obvious that reliable and sensitive analytical methods for the determination of N_2H_4 are needed.

Here, we report the synthesis of nickel oxide nanoparticles using an anionic surfactant and gelatin. The nickel oxide nanoparticles were characterized by UV–vis, SEM, XRD and TEM methods. Nickel oxide nanoparticles were applied as a catalyst in the decomposition reaction of hydrazine.

EXPERIMENTAL

Gelatin from bovine skin, hydrazine hydrate, nickel chloride and sodium dodecyl sulphate (SDS) were purchased from Aldrich. All solutions were prepared using redistilled water. Other reagents were of analytical grade and were purchased from Aldrich or Merck and were used as received without further purification.

All spectroscopic experiments were performed on a UV–vis absorbance spectrophotometer (Shimadzu, Kyoto, Japan). All experiments were carried out at room temperature. TEM images were recorded using a LEO-Libra 120 transmission electron microscope. Hitachi S-3500N scanning electron microscope (SEM) was used for surface image measurements. The crystallization and purity of the synthesized samples were characterized by X-ray diffraction.

5 g of gelatin was dissolved in 100 mL of deionized water and was stirred at 60 ˚C for 30 min to achieve a clear gelatin solution. 10 mL of SDS surfactant solution (2 M) and 10 mL of nickel chloride solution (1 M) were added to the above solution under continuous stirring, after which the container was placed in a water bath. The temperature of the water bath was fixed at 80 ˚C. The stirring was continued for 3 h. The final product was placed in a furnace at a temperature of 500 ˚C for 8 h to obtain NiO nanoparticles. The yield of NiO nanoparticles calculated by weighing the produced NiO nanoparticles was found to be 81 and 85% for NiO nanoparticles synthesized in absence and presence of SDS, respectively.

RESULTS AND DISCUSSION

Fig. 1 shows the XRD pattern of the NiO-NPs prepared using gelatin in absence and presence of SDS. The dominant peaks for NiO-NPs were identified at about 2θ = 37, 43, 62, 75 and 79; they were indexed as (111), (200), (220), (311), and (222), respectively, according to JCPDS reference number 078-0643.

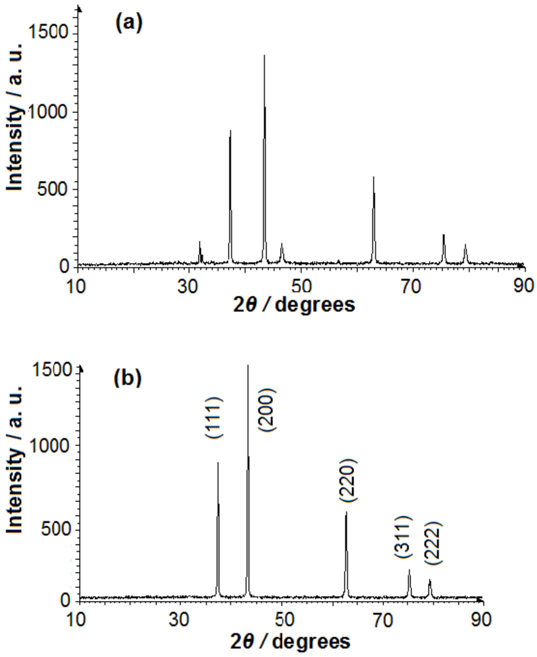

Fig. 1. XRD patterns of NiO-NPs synthesized in absence (a) and presence of SDS (b).

The average particle size of pure NiO-NPs was derived from the high intensity diffraction peak in Fig. 1, using Debye Scherrer's formula: $D = K\lambda / \beta\cos\theta$, where D is the crystallite size, K the Scherrer constant usually taken as 0.89, λ is the wavelength of the X-ray radiation (0.15418 nm for Cu Ka), and β is the full width half maximum of the diffraction peak measured at 2θ (β for 43 value of 2θ is 0.61 and 0.45 for NiO-NPs powder synthesized in presence and absence of SDS, respectively). The average crystallite size of NiO-NPs synthesized in presence and absence of SDS was found to be approximately 14 and 19 nm, respectively. It is clear from the crystalline sizes that the SDS plays a major role in the synthesis of NiO nanoparticles and most probably controls the growth of nanoparticles by preventing their agglomeration. SDS (with negative charge) adsorbs Ni^{+2} ions *via* electrostatic force and prevents nanoparticles to get aggregated *via* coulombic repulsion and steric hindrance.

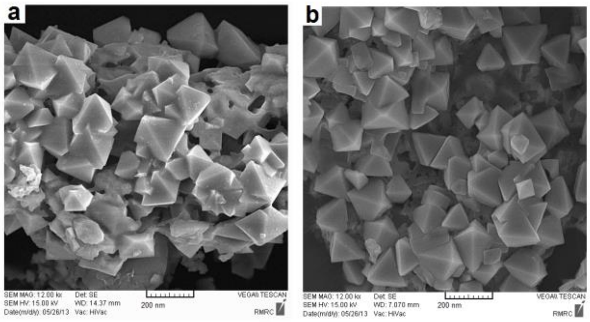

Fig. 2. SEM images of NiO-NPs synthesized in absence (a) and presence of SDS (b)

Fig. 2 shows the SEM images of the NiO nanoparticles synthesized using gelatin in presence and absence of SDS. It can be seen from the SEM image that the products are trigonal-shaped. The presence of SDS decreased the average size of the synthesized NiO particles (Fig. 2b) and the particles were uniform while without SDS, some particles were amorphous-shaped and had high size distribution (Fig. 2a).

EDAX results (Fig. 3) confirmed the presence of Ni and O elements in nanoparticles synthesized using gelatin in absence and presence of SDS.

Fig. 4 shows the TEM images and size histograms of the NiO nanoparticles synthesized using gelatin in presence and absence of SDS. According to the TEM analysis data and the size distribution plots, the small size of particles is generated by SDS surfactant. The obtained particle sizes from the TEM were in good agreement with those calculated from XRD analysis.

The optical absorption of suspended NiO nanoparticles was measured in the 200–600 nm wavelength range. Prior to the measurements of UV–vis absorption, the powder samples (2 mg/mL) were uniformly and gently dispersed in methanol solvent.

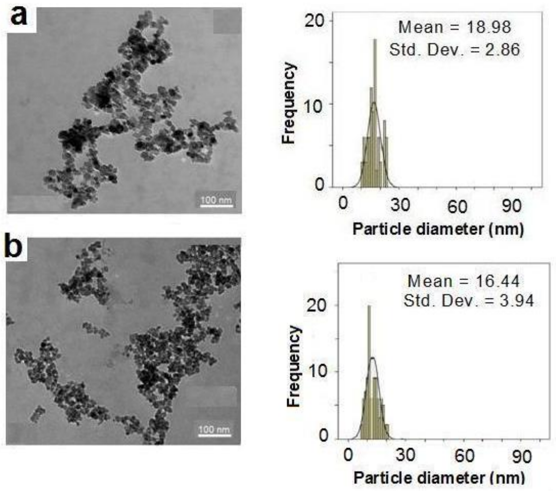

Fig. 4. TEM images and histograms of NiO-NPs synthesized in absence (a) and presence of SDS (b).

The UV–vis absorption spectra of the NiO nanoparticles at room temperature are depicted in Fig. 5.

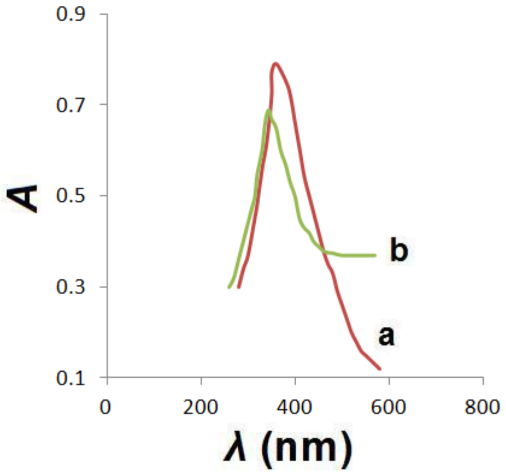

Fig. 5. UV-Vis patterns of NiO-NPs synthesized in absence (a) and presence of SDS (b).

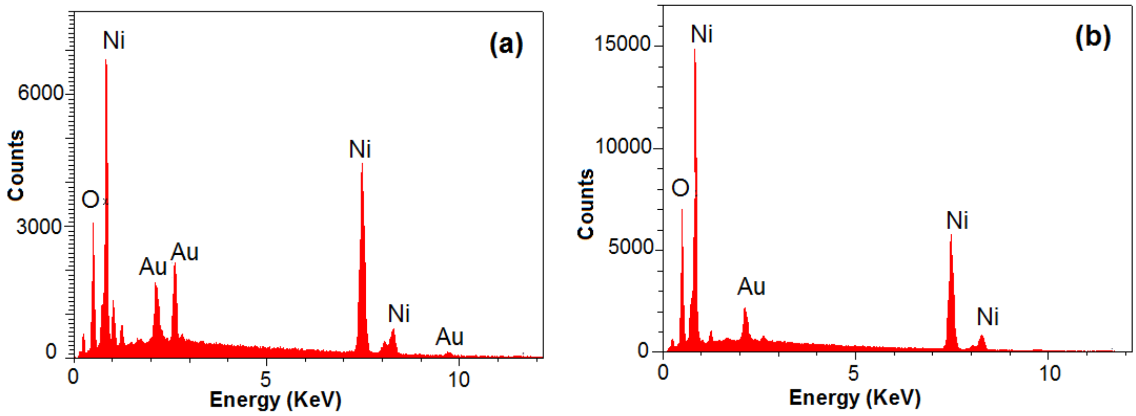

Fig. 3. EDAX images of NiO-NPs synthesized in absence (a) and presence of SDS (b).

Table 1. Compared parameters of NiO-NPs synthesized using different methods.

Method	Agent	Particle size (nm)	Synthesis temperature (˚C)	Reference
Chemical	Sodium borohydride	20-40	500	[29]
Spray pyrolysis	Silica matrix	55	500	[30]
Soft-templating	Poly(propylene oxide)- poly(ethylene oxide)	31	400	[31]
Microemulsion	Tween 80	100-160	-	[32]
Sol-gel	SDS	16	500	This work

The band position of NiO prepared in absence of SDS (curve a) at around 370 nm corresponds to NiO nanoparticles. SDS (curve b) causes a shift of the band to almost 360 nm. This blue shift indicates the quantum confinement property of nanoparticles. In the quantum confinement range, the band gap of the particle increases which results in a shift of the absorption edge to lower wavelength, as the particle size decreases.

The band gap energy (*E*) was calculated according to the literature report [28] using the following equation:

$$\text{Band gap energy } (E) = hc/\lambda \qquad (1)$$

where h is the Plank's constant, 6.626×10^{-34} J s, c is the speed of light, 3.0×10^{8} m/s; λ is the wavelength (nm). According to this equation, the band gap of NiO-NPs synthesized without surfactant is 3.4 eV and the band gap of synthesized NiO-NPs using SDS is 3.6 eV. These results confirm that when the size is smaller, the band gap will be larger.

The proposed method for synthesis of NiO nanoparticles was compared with those reported in the literature, as given in Table 1 [29-32]. As can be seen from Table 1, the present method is comparable with those reported in the literature. The catalytic decomposition reaction of hydrazine hydrate was studied in the presence of nickel oxide nanoparticles in aqueous medium. An aqueous solution of hydrazine (pH 7.00) has an adsorption peak at 293 nm (Fig. 6).

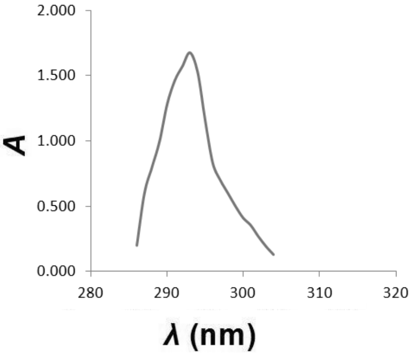

Fig. 6. UV-Vis pattern of 0.25 mM hydrazine in aqueous solution.

In a set of experiments, 2 mg of nickel oxide nanoparticles was added to a hydrazine aqueous solution (0.25 mM, 5 mL), and the reaction temperature was maintained at 25 ˚C. The intensity of hydrazine in presence of nickel oxide nanoparticles keeps on decreasing with time (Fig. 7).

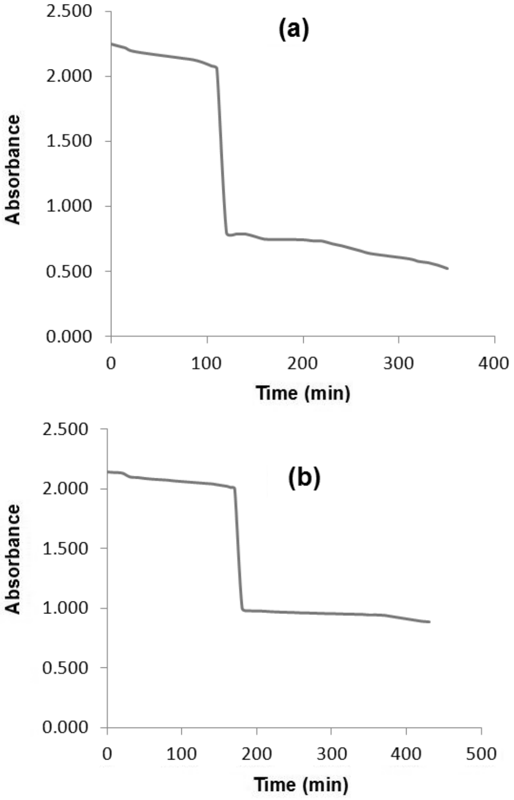

Fig. 7 Plot of absorbance *vs*. time for the decomposition of hydrazine in presence of NiO-NPs as catalyst; conditions: (a) 0.25 mM hydrazine (5 ml) and (b) 0.25 mM hydrazine plus NiO-NPs (2 mg), at 25 ˚C.

There is no considerable change in intensity of the absorption peak in hydrazine solution without nickel oxide nanoparticles (not shown), indicating that its concentration in the reaction mixture remains almost constant and no decomposition reaction takes place in the absence of NiO nanoparticles as a catalyst. This study shows that nanoparticles have large active surface area for the decomposition reaction. For the evaluation of the catalytic rate of hydrazine decomposition reaction, pseudo-first-order kinetics with respect to hydrazine can be used. The role of metal nanoparticles is very important in redox reactions. Hydrazine hydrate is readily soluble in water; since N_2H_4 is basic, the chemically active free ion is normally represented as $N_2H_5^+$ [33]:

$$N_2H_4.H_2O \leftrightarrow N_2H_5^+OH^- \qquad (1)$$

Accordingly, it was clearly shown that hydrazine could be catalytically decomposed into hydrogen and nitrogen by nickel nanoparticles. The decomposition reaction is [34]:

$$N_2H_5^+OH^- \leftrightarrow N_2 + 2H_2 + H_2O \qquad (2)$$

The decomposition process involves chemisorption of hydrazinium ions onto the NiO nanoparticles surface, and interfacial electron transfer released by the hydrazinium ion [35].

As shown in Fig. 7, hydrazine decomposition rate in presence of NiO-NPs synthesized using SDS is high as compared to those synthesized without SDS. These results confirm that when the particle size is smaller, the active surface area for decomposition reaction is larger and the catalytic rate of hydrazine decomposition reaction increases. From the linear relationship between the amount of hydrazine decomposed and reaction time, the decomposition rate of hydrazine in presence of NiO-NPs synthesized in presence and absence of SDS was estimated to be 9.1 and 4.2 nmol/(min mg of NiO-NPs), respectively.

The NiO nanocatalyst was found functional after completion of the decomposition process. The particles were separated from the reaction mixture, washed with deionized water and vacuum-dried. These particles were reused at least 3 times for the same decomposition reaction. Every time, nearly the same reaction time was observed. So we concluded that the NiO nanoparticles were not poisoned.

CONCLUSIONS

Nickel oxide nanoparticles were synthesized from nickel chloride using gelatin in presence of SDS. The resultant nanoparticles were characterized by XRD, TEM, SEM and UV-Vis spectroscopy. The XRD results showed a pure nickel oxide crystalline phase with crystallite size about 14 nm, which agrees well with the TEM results. The catalytic decomposition reaction of hydrazine hydrate was studied in the presence of nickel oxide nanoparticles in aqueous medium. It was observed that hydrazine was catalytically decomposed into hydrogen and nitrogen gases by nickel oxide nanoparticles. The decomposition rate at 25 °C was estimated to be 9.1 nmol/(min mg of NiO-NPs).

REFERENCES

1. S. A. Majetich, Y. Jin, *Science*, **284**, 470 (1999).
2. A. J. Zarur, J. Y. Ying, *Nature*, **403**, 65 (2000).
3. Y. Xia, P. Yang, Y. Sun, Y. Wu, B. Mayers, B. Gates, Y. Yin, F. Kim, H. Yan, *Adv. Mater.*, **15**, 353 (2003).
4. T. Prozorov, G. Kataby, R. Prozorov, A. Gedanken, *Thin Solid Films*, **340**, 189 (1999).
5. J. H. Lee, B. E. Park, Y. M. Lee, S. H. Hwang, W. B. Ko, *Current Applied Physics*, **9,** 152 (2009).
6. C. Wang, Y. Hu, C. M. Lieber, S. Sun, *J. Am. Chem. Soc.*, **130**, 8902 (2009).
7. C. S. Levin, J. Kundu, A. Barhoumi, N. J. Halas, *Ananlyst*, **134**, 1745 (2009).
8. N. H. Kim, S. J. Lee, M. Moskovits, *Nano Lett.*, **10**, 4181 (2010).
9. M. P. Murray-Methot, M. Ratel, J. F. Masson, *J. Phys. Chem. C*, **114**, 8268 (2010).
10. G. Li, J. Zhai, D. Li, X. Fang, H. Jiang, Q. Dong, E. Wang, *J. Mater. Chem*., **20**, 9215 (2010).
11. M. P. Pileni, *Adv. Funct. Mater*., **11**, 323 (2001).
12. S. Sun, C. B. Murray, D. Weller, L. Folks, A. Moser, *Science*, **287**, 1989 (2000).
13. V. B. Vladimir, N. M. Valentin, V. G. Nikolay, *Chem. Vap. Deposion.*, **11**, 368 (2005).
14. Q. Zhen-ping, G. Hong-xia, L. Dong-sheng, Sh. Xue-ping, *J. Func. Mater. Devices*, **10**, 95 (2004).
15. H. E. Yuan-qing, L. I. Xue-geng, M. T. Swihart, *Chem. Mater.*, **17**, 1017 (2005).
16. L. Zhao-ping, L. Shu, Y. You, P. Sheng, H. Zhao-kang, Q. Yi-tai, *Adv. Mater.*, **15**, 1946 (2003).
17. L. Yun-jun, L. Wei-ping, W. Xian-ni, *West Leacher*, **2**, 20 (2002).
18. Z. Khan, O. Bashir, J. I. Hussain, S. Kumar, R. Ahmad, *Colloids Surf. B: Biointerfaces*, **98**, 85 (2012).
19. W. Wang, B. Gu, L. Liang, *J. Colloid Interf. Sci*., **313**, 169 (2007).
20. S. Hosseini, W. R. Wan Daud, M. Badiei, A. A. Hassan Kadhum, A. B. Mohammad, *Bull. Mater. Sci.*, **34**, 759 (2011).
21. Q. A. Drmosh, M. A. Gondal, Z. H. Yamani, T. A. Saleh, *Applied Surface Science*, **256**, 4661 (2010).
22. S. K. Mehta, S. Kumar, S. Chaudhary, K. K. Bhasin, *Nanoscale Res. Lett*., **4**, 1197 (2009).
23. B. Tah, P. Pal, M. Mahato, G. B. Talapatra, *J. Phys. Chem. B*, **115**, 8493 (2011).
24. Sh. G. Dixit, A. R. Mahadeshwar, S. K. Haram, *Colloids and Surfaces A: Physicochemical and Engineering Aspects*, **133**, 69 (1998).
25. B. K. Jena, C. R. Raj, *J. Phys. Chem. C*, **111**, 6228 (2007).
26. Y. He, J. Zheng, Q. Sheng, *Microchim Acta*, **177**, 479 (2012).
27. B. Fang, R. X. Shen, W. Zhang, G. F. Wang, C. H. Zhang, *Microchim Acta*, **165**, 231 (2009).
28. M. Hoffman, S. Martin, W. Choi, D. Bahnemann, *Chem. Rev*., **95**, 69 (1995).

29. Zh. You-xian, F. Wen-jie, A. Xue-qin, *Trans. Nonferrous Met. Soc. China*, **18**, 212 (2008).
30. H. S. Kim, Ch. S. Kim, S. G. Kim, *J. Non-Crystalline Solids*, **352**, 2204 (2006).
31. J. Choma, K. Jedynak, M. Marszewski, M. Jaroniec, *Applied Surface Science*, **258**, 3763 (2012).
32. A. T. Shah, M. I. Din, et al., *Colloids and Surfaces A: Physicochem. Eng. Aspects*, **405**, 19 (2012).
33. M. L. Singla, A. Negi, V. Mahajan, K. C. Singh, D. V. S. Jain, *Applied Catalysis A: General*, **323**, 51 (2007).
34. A. Salimi, R. Hallaj, S. Soltanian, *Biophysical Chemistry*, **130**, 122 (2007).
35. S. H. Wu, D. H. Chen, *J. Colloid & Interf. Sci*., **259**, 282 (2003).

РАЗГРАЖДАНЕ НА ХИДРАЗИН, КАТАЛИЗИРАНО ОТ НАНО-ЧАСТИЦИ ОТ НИКЕЛОВ ОКСИД ПРИ СТАЙНА ТЕМПЕРАТУРА

Ф. Чекин *, С. Садеги

Департамент по химия, Ислямски университет „Азад“, Клон “Аятолах Амоли“, Амол, Иран

Постъпила на 27 април, 2014 г., коригирана на 1 септември, 2014 г.

(Резюме)

В тази работа се съобщава за прост и евтин метод за синтезата на нано-частици никелов оксид (NiO-NPs) използвайки натриев доцецил-сулфат (SDS) и желатин като стабилизатор. Синтезираните NiO-NPs са оарактеризирани с трансмисионна електрон-микроскопия (TEM), прахова рентгенова дифракция (XRD), сканиаща електрон-микроскопия (SEM) и UV-vis спектроскопия. Резултатите показват, че по този прост метод са получени NiO-наночастици с висока кристалинност. Размерът на зърната, определени с TEM е 16 nm в присъствие на, което се съгласува добре с XRD-данните. SDS има важно значение за формиране на NiO-наночастиците. Тези часици са използвани като твърдо-фазен катализатор при разлагането на хидразин при стайна температура. Процесът на разлагане е наблюдаван чрез UV–vis анализ. Изследването показва, че наночастиците не се отравят при многократна употреба при разлагането на хидразин. Намерено е, че хидразинът се разлага на газообразни водород и азот. Скоростта на разлагане при 25 °C е 9.1 nmol/(min mg of NiO-NPs).